

# Sequential Nutrient Uptake by Phytoplankton Maintains High Primary Productivity and Balanced Nutrient Stoichiometry

Kedong Yin<sup>1,2\*</sup>, Hao Liu<sup>1,2#</sup> and Paul J. Harrison<sup>3</sup>

- [1]{School of Marine Sciences, Sun Yat-sen University, Guangzhou, China}
- [2]{Key Laboratory of Marine Resources and Coastal Engineering in Guangdong Province, Guangzhou, China}
- [3]{Department of Earth and Ocean Sciences, University of British Columbia, Vancouver BC V6T 1Z4}

\*Correspondence to: Kedong Yin, School of Marine Science, Sun Yat-sen University (East Campus), Guangzhou Higher Education Mega Center, Guangzhou, 510006, China.

Tel. +86 (0)20 3933 6536; Fax +86 (0)20 3933 6607. E-mail [yinkd@mail.sysu.edu.cn](mailto:yinkd@mail.sysu.edu.cn)

#Joint first author

Running head: sequential nutrient uptake, nutritional strategy, nutrient stoichiometry

26 **Abstract**

27 We hypothesize that phytoplankton have the sequential nutrient uptake strategy to  
28 maintain nutrient stoichiometry and high primary productivity in the water column.  
29 Phytoplankton take up the most limiting nutrient first until depletion, continue to drawdown  
30 non-limiting nutrients and then take up the most limiting nutrient rapidly when it is available.  
31 The processes result in the variation of ambient nutrient ratios in the water column around the  
32 Redfield ratio. We used high resolution continuous vertical profiles of nutrients, nutrient  
33 ratios and on-board ship incubation experiments to test this hypothesis in the Strait of  
34 Georgia. At the surface in summer, ambient  $\text{NO}_3^-$  was depleted with excess  $\text{PO}_4^{3-}$  and  $\text{SiO}_4^{4-}$   
35 remaining, and as a result, both N:P and N:Si ratios were low. The two ratios increased to  
36 about 10:1 and 0.45:1, respectively, at 20 m. Time series of vertical profiles showed that the  
37 leftover  $\text{PO}_4^{3-}$  continued to be removed, resulting in additional phosphorus storage by  
38 phytoplankton. There were various shapes of vertical profiles of N:P and at the nutricline in  
39 response to mixing events. A field incubation of seawater also demonstrated the sequential  
40 uptake of  $\text{NO}_3^-$  (the most limiting nutrient) and then  $\text{PO}_4^{3-}$  and  $\text{SiO}_4^{4-}$  (the non-limiting  
41 nutrients). This sequential uptake strategy allows phytoplankton to acquire additional cellular  
42 phosphorus and silicon when they are available and wait for nitrogen to become available  
43 through frequent mixing of  $\text{NO}_3^-$  (or pulsed regenerated  $\text{NH}_4^+$ ). Thus, phytoplankton subject to  
44 the homeostatic stoichiometry of nutrients and are capable of maintaining high productivity  
45 by taking advantage of vigorous mixing regimes. To our knowledge, this is the first study to  
46 show the in situ dynamics of continuous vertical profiles of N:P and N:Si ratios and to  
47 examine the responses of phytoplankton to nutrients supplied naturally by mixing events.  
48 This provided insight into the in situ dynamics of nutrient stoichiometry in the water column  
49 and the inferring of the transient status of phytoplankton nutrient stoichiometry in the coastal  
50 ocean.

51     **1. Introduction**

52         The stoichiometry of the C:N:P Redfield ratio (Redfield, 1958) remains a central  
53         tenet in oceanography as it couples ecosystem processes with ocean biogeochemistry, which  
54         is driven by physical processes in oceans. Redfield ratio of C:N:P varies widely across a wide  
55         range of environmental conditions. Laboratory cultures of phytoplankton that are in the  
56         steady state usually display variable cellular N:P ratios with the nutrient N:P supply ratios  
57         (Geider and La Roche, 2002). Recently, Martiny et al. (2013) found strong latitudinal patterns  
58         of the elemental ratios, which are closely related with ambient levels of nutrients in these  
59         waters by making comparative analysis of elemental ratios of organic matter between  
60         different latitudes. Even at a fixed site, the Bermuda Atlantic Time-Series Study Station in  
61         the North Atlantic Ocean, C: N: P ratio is quite variable (Singh et al. 2015). Four mechanisms  
62         have been proposed to explain the variability in C:N:P ratios in marine plankton, as  
63         summarized by Weber and Deutsch (2010). The first mechanism emphasizes the relationship  
64         between cellular elemental stoichiometry of phytoplankton and ambient nutrient ratios, i.e.,  
65         the stoichiometry of nutrients in the water column. Based on the average Redfield ratio, this  
66         mechanism has been used to infer the most limiting nutrient for phytoplankton and to debate  
67         which nutrient, nitrogen or phosphorus, should be managed to control eutrophication effects.  
68         The second mechanism suggests that the elemental stoichiometry is taxonomy specific.  
69         Diatoms were reported to drawdown nutrients with a low nutrient C:P and N:P ratios (Geider  
70         and La Roche, 2002; Elser et al., 2003; Price, 2005), while marine cyanobacteria have higher  
71         C:P and N:P ratios (Karl et al., 2001; Bertilsson et al., 2003). Such different uptake ratios of  
72         N:P by phytoplankton can influence the magnitude of ocean N-fixation (Mills and Arrigo  
73         2010) Based on the resource allocation theory, the third proposed mechanism is the “growth  
74         rate hypothesis”, which states that the elemental stoichiometry within a cell is controlled by  
75         the biochemical allocation of resources to different growth strategies (Falkowski, 2000; Elser

76 et al., 2003; Klausmeier et al., 2004). Fast-growing cells may have a lower N:P ratio due to a  
77 larger allocation to P-rich assembly machinery of ribosomes (Loladze and Elser, 2011),  
78 whereas competitive equilibrium favors a greater allocation to P-poor resource acquisition  
79 machinery and therefore, higher N:P ratios. The fourth mechanism is related to the  
80 interference from dead plankton or organic detritus with the measurement of elemental  
81 composition of organic matter, but such interference cannot be assessed since there is lack of  
82 the measurements of non-living organic matters in oceans and coastal waters.

83 In culture experiments, continuous uptake of non-limiting nutrients has been  
84 demonstrated for diatoms under N and Si limitation (Conway et al., 1976; Conway and  
85 Harrison, 1977; Harrison et al., 1989). Surge uptake of the limiting nutrient occurs when it is  
86 added to the nutrient starved phytoplankton culture, while the uptake of the non-limiting  
87 nutrient is slowed or stopped until the diatom has overcome its nutrient debt. Hence, the  
88 sequence of which nutrient is taken up first is directly related to the nutrient status of the  
89 phytoplankton. It is difficult to assess the nutritional status of phytoplankton in the field, but  
90 the application of laboratory results to the interpretation of vertical nutrient profiles can  
91 provide information on their nutritional status. To date, there have been no studies of  
92 sequential uptake of nutrients in the field using a series of high resolution vertical profiles of  
93 nutrients and their application to nutritional status of the phytoplankton.

94 In this study, we used high resolution continuous vertical profiles of N:P and N:Si  
95 ratios to examine how N:P and N:Si ratios respond to the mixing in a highly dynamic coastal  
96 water column and the uptake of nutrients. On-board ship incubation experiments were  
97 conducted to support the observations of changes in vertical profiles of N:P and N:Si ratios.  
98 We constructed seven conceptual profiles to illustrate how a vertical profile of N:P ratios  
99 changes with mixing and uptake of nitrogen and phosphorus and how they could indicate the  
100 nutritional status of the phytoplankton assemblage. The conceptual model also explains how

101 N:P ratios respond to mixing, particularly at the nutriclines (nitracline for  $\text{NO}_3^-$ , phosphacline  
102 for  $\text{PO}_4^{3-}$  and silicacline for  $\text{SiO}_4^{4-}$ ), and indicates which nutrient,  $\text{NO}_3^-$  or  $\text{PO}_4^{3-}$ , is taken up  
103 first in the water column. To our knowledge, this is the first study to show the dynamics of  
104 continuous vertical profiles of N:P and N:Si ratios and to examine the nutritional status of  
105 phytoplankton and their response to the supply of nutrients from water column mixing. We  
106 believe that our approach can add a new dimension to examining the in situ dynamics of  
107 nutrients in the water column and illustrate the ecological role of phytoplankton  
108 stoichiometry in phytoplankton competition for nutrients.

### 109 **1.1. Conceptual Model of Variability in Vertical N:P ratios**

110  
111 The Strait of Georgia (hereafter the Strait) is an inland sea that lies between Vancouver Island  
112 and the mainland of British Columbia (LeBlond 1983). It is an ideal area for studying the  
113 interactions between mixing, nutrient vertical profiles and phytoplankton nutrient uptake  
114 because of its relatively high biomass, frequent wind mixing and shallow (15 m) photic zone.  
115 The Strait is biologically productive, reaching as as daily production up to  $5 \text{ g C m}^{-2} \text{ day}^{-1}$  and  
116 annual about  $>300 \text{ g C m}^{-2} \text{ yr}^{-1}$  (Harrison et al., 1983, 1991), but inorganic nitrogen is often  
117 undetectable in productive seasons in the surface layer. The nutricline sitting within the  
118 euphotic zone is often associated with the pycnocline. In the Strait, the ambient N:P ratio of  
119 nutrients is  $\sim 10:1$ , similar to other coastal areas (Hecky and Kilham, 1988).

120 We illustrate the conceptual model of variability in vertical profiles of N:P ratios based  
121 on seven (C0 to C6) vertical profiles that we encountered in our field studies and suggest  
122 events that likely occurred to produce these nutrient profiles (Fig. 1).

123 **C0:** in winter or after a strong wind speed event, the water column is homogeneously  
124 mixed, and  $\text{NO}_3^-$  and  $\text{PO}_4^{3-}$  are uniformly distributed in the water column. **C1:** with the onset  
125 of stratification,  $\text{NO}_3^-$  and  $\text{PO}_4^{3-}$  are taken up within the mixed layer. Assuming that the  
126 average nutrient uptake ratio is 16N:1P, a N:P uptake ratio that is  $>10:1$  would decrease the

127 ambient N:P ratio to <10:1. **C2:** the uptake of  $\text{NO}_3^-$  and  $\text{PO}_4^{3-}$  proceeds at a N:P ratio >10:1  
128 until  $\text{NO}_3^-$  is just depleted. At this time the N:P ratio is near 0 and some  $\text{PO}_4^{3-}$  remains in the  
129 water column. **C3:** the remaining  $\text{PO}_4^{3-}$  is completely taken up and stored as extra/surplus  
130 intracellular  $\text{PO}_4^{3-}$ . **C4:** after cross-pycnocline mixing occurs, the ambient N:P ratio in the  
131 newly mixed water should be the same as the ratio in the deep water. As a result, the vertical  
132 profile of the N:P ratio will form a right angle on the top part of the nutricline. **C5:** depending  
133 on how long the phytoplankton are nutrient limited, their response to the mixed limiting  
134 nutrient can be different. When N deficient phytoplankton take up N only, the curve of the  
135 N:P ratio parallels the  $\text{NO}_3^-$  distribution curve and  $\text{PO}_4^{3-}$  is left behind in the water column.  
136 **C6:** on the other hand, if phytoplankton take up  $\text{PO}_4^{3-}$  before  $\text{NO}_3^-$  (e.g. if phytoplankton  
137 were severely N starved, and there is a lag in  $\text{NO}_3^-$  uptake), the N:P ratio would be higher at  
138 the nutricline than below (Fig. 1).

139 Similarly, this conceptual model can be applied to N,  $\text{SiO}_4^{4-}$  and N:Si ratios. The  
140 ambient (N:Si) ratio is about 0.5:1 at 20 m in the Strait, with 20  $\mu\text{M}$   $\text{NO}_3^-$  and 40  $\mu\text{M}$   $\text{SiO}_4^{4-}$ .  
141 As the average uptake ratio of N:Si is about 0.7-1:1 (equivalent to Si:N = 1.5-1:1)  
142 (Brzezinski, 1985), the N:Si ratio decreases with depth.  $\text{SiO}_4^{4-}$  is rarely depleted and  
143 therefore, the N:Si ratio is mainly determined by the distribution of  $\text{NO}_3^-$ . The continuous  
144 uptake of  $\text{SiO}_4^{4-}$  without the uptake of  $\text{NO}_3^-$  can be inferred based on the comparison between  
145 the gradient of N:Si and the silicacline. For example, a sharper gradient of the N:Si ratio than  
146 the silicacline would indicate the continuous uptake of  $\text{SiO}_4^{4-}$  without the uptake of  $\text{NO}_3^-$  as in  
147 C5 (Fig. 1)

148 **2. Materials and Methods**

149 **2.1. Station Locations**

150 The transect started from station S2, 8 km beyond the Fraser River mouth and under  
151 the influence of the river plume and extended 108 km NW to S1 (well beyond the plume) in

152 the Strait of Georgia (Fig. 2). The station numbers are consistent with previous studies (Yin et  
153 al., 1997a).

154 **2.2. Sampling and Data Processing**

155 The sampling was designed to investigate the distribution of nutrients ( $\text{NO}_3^-$ ,  $\text{PO}_4^{3-}$   
156 and  $\text{SiO}_4^-$ ) and N:P and N:Si ratios associated with mixing processes during August 6-14,  
157 1991. Data at either an anchored station for 24 h, or a transect of a few stations within 10 h  
158 was used. At each station, a vertical profile (0-25 m) of temperature, salinity, *in vivo*  
159 fluorescence and selected nutrients ( $\text{NO}_3^- + \text{NO}_2^-$ ,  $\text{PO}_4^{3-}$  and  $\text{SiO}_4^-$ ) were obtained. Only  
160 vertical profiles of nutrients are presented in this study. Other data (salinity, temperature and  
161 fluorescence) are published elsewhere (Yin et al., 1997a). The vertical profiling system has  
162 been described in detail by Jones et al. (1991) and Yin et al. (1995a). Basically, a hose  
163 connected to a water pump on deck was attached to the CTD probe or S4 (InterOcean<sup>®</sup>)  
164 which has the dual function of a CTD probe and a current meter. Seawater from the pump  
165 was connected into the sampling tubing of an AutoAnalyzer<sup>®</sup> on board ship for *in situ*  
166 nutrient measurements, while the CTD probe was lowered slowly into the water at  $1 \text{ m min}^{-1}$ .  
167 Each sampling produced a high resolution continuous vertical profile of physical and  
168 biological parameters and thus the relationship between these parameters in the water column  
169 can be easily recognized. Data from a vertical profile (a datum point every 3 s) were  
170 smoothed over 15 s intervals. This smoothing reduced the fluctuations caused by ship's  
171 motion.

172 **2.3. Analysis of Nutrients**

173 All nutrients were determined using a Technicon AutoAnalyzer II. Salinity effects on  
174 nutrient analyses were tested on board ship and were found to be small. Therefore, no  
175 correction was made for salinity effects.  $\text{NO}_3^- + \text{NO}_2^-$  and  $\text{PO}_4^{3-}$  were determined following the

176 procedures of Wood et al. (1967) and Hager et al. (1968), respectively. The analysis of  $\text{SiO}_4^{4-}$   
177 was based on Armstrong et al. (1967) and ammonium analysis followed Parsons et al. (1984). A water  
178 sample for particulate organic carbon and nitroeng (POC and PON) was filtered onto a GF/F filter  
179 and POC/PON on the filter were analyzed with a Carlo Erba model NA 1500 NCS elemental  
180 analyzer, using the dry combustion method described by Sharp (1974).

181 **2.4. Field Incubation Experiments**

182 Niskin bottles (5 L) were used to take seawater samples and the samples were  
183 transferred to acid cleaned carboys (10 L). Subsamples of seawater were transferred to  
184 transparent polycarbonate flasks (1 L) and placed in Plexiglas tanks. The tanks were kept at  
185 the same temperature as the surface water by pumping seawater (from the ship's intake at 3  
186 m) through the tank. The incubation flasks were wrapped with 1 or 4 layers of neutral density  
187 screening which corresponded to the light intensity from which the samples were taken (1 or  
188 16 m). In the nutrient enrichment experiments,  $\text{NO}_3^-$ ,  $\text{PO}_4^{3-}$  and  $\text{SiO}_4^{4-}$  were added to the  
189 samples, yielding final 20-30, 2-3 and 20-30  $\mu\text{M}$ , respectively. The incubations lasted for 24  
190 or 96 h, and subsamples were taken every 3-6 h for measurements of fluorescence and  
191 nutrients. The incubation experiments were conducted in different years, but in the same  
192 season.

193 **3. Results**

194 **3.1. Vertical Profiles of Nutrients and Nutrient Ratios**

196 At S3 near the edge of the Fraser River plume, the profiles documented changes  
197 before (T1) and after wind mixing (T7). At T1, both  $\text{NO}_3^-$  and  $\text{PO}_4^{3-}$  were low in the surface  
198 layer and N:P ratios were low (<2:1) and increased to ~8:1 at 20 m (Fig. 3). At T7, higher N:P  
199 ratios of 16-20:1 occurred due to an increase in  $\text{NO}_3^-$  in the deep water.  $\text{SiO}_4^{4-}$  was ~30  $\mu\text{M}$  at  
200 the surface due to input from the Fraser River, and increased to 37  $\mu\text{M}$  at 20 m (Fig. 3). The  
201 N:P ratio curve nearly formed a right angle at the top of the nutriclines at T7 when the

202 gradient of the nitracline was larger than that of the phosphacline. At T1, the N:Si ratio was  
203 near 0 because  $\text{NO}_3^-$  was near the detection limit, but started to increase along the nitracline  
204 at the depth of the  $\text{SiO}_4^{4-}$  minimum. At T7, N:Si increased more rapidly with the nitracline.

205 A strong wind speed event occurred on August 7 and the water column was mixed  
206 (Yin et al., 1997b). We followed the change in the nutrient profiles and nutrient ratios from  
207 S3 near the Fraser River plume, to P4 and P6 and the well beyond the plume to S1. At S3,  
208 N:P ratios in the water column were  $>7:1$  when both  $\text{NO}_3^-$  and  $\text{PO}_4^{3-}$  were high after wind  
209 mixing, with N:Si ratios being  $<0.5:1$  (Fig. 4). As the post-wind bloom of phytoplankton  
210 developed along P4-P6 due to the newly supplied nutrients (Yin et al., 1997b), N:P ratio  
211 followed the distribution of  $\text{NO}_3^-$  at P4, and decreased to 0 as  $\text{NO}_3^-$  was depleted at the  
212 surface at P6 (Fig. 4). It was clear that little  $\text{PO}_4^{3-}$  was consumed while  $\text{NO}_3^-$  was taken up. At  
213 the same time, the silicacline deepened and paralleled the nitracline. At S1, N:P and N:Si  
214 ratios formed almost a vertical line. N:P and N:Si ratios were  $\sim 8:1$  and  $0.5:1$ , respectively, in  
215 the deep water (Fig. 4).

216 The time series (T1, T3, T8 and T11) of Aug 8-9 captured changes over 1 or 2 days  
217 after the wind mixing event at S1 that was well beyond the river plume (Fig. 5). At T1, N:P  
218 and N:Si ratios were  $\sim 9:1$  and  $0.45:1$ , respectively, with  $\text{NO}_3^-$  and  $\text{PO}_4^{3-}$  being  $15$  and  $1.7 \mu\text{M}$ ,  
219 respectively, at the surface. At T3, N:P ratio remained constant at  $\sim 9:1$ , while  $\text{NO}_3^-$  and  $\text{PO}_4^{3-}$   
220 decreased by  $10$  and  $1.0 \mu\text{M}$ , respectively, indicating an uptake N:P ratio of  $10:1$ . In  
221 comparison, N:Si ratio decreased from T1 to T3 when  $\text{SiO}_4^{4-}$  was  $35 \mu\text{M}$  at T1 and decreased  
222 by  $>10 \mu\text{M}$  at T3, producing an uptake N:Si ratio of  $\sim 1:1$ . At T8, N:P ratio followed the  $\text{NO}_3^-$   
223 distribution as  $\text{NO}_3^-$  decreased to  $\sim 0 \mu\text{M}$  at the surface while  $\text{PO}_4^{3-}$  was still  $\sim 0.5 \mu\text{M}$ . This  
224 indicated that  $\text{NO}_3^-$  uptake was more rapid than  $\text{PO}_4^{3-}$  uptake and hence  $\text{NO}_3^-$  mainly  
225 determined the ambient N:P ratios. The N:Si uptake ratio of  $\sim 1:1$  continued until T8.

226 However, at T11, the N:P ratio spiked higher in the top 5-10 m of the nutricline, suggesting a  
227 more rapid uptake of  $\text{PO}_4^{3-}$  relative to  $\text{NO}_3^-$  in the upper portion of the phosphacline (Fig. 5).

228 Changes in the profiles after the wind event on Aug 7 were followed over 5 days (Aug  
229 10 – 14) at P5 that was still within the influence of the river plume as evidenced by the higher  
230 surface  $\text{SiO}_4^{4-}$  at the surface (Fig. 6). On Aug 10-11, N:P ratios were higher at the surface  
231 where the post-wind induced bloom occurred two days earlier, suggesting that uptake of  
232  $\text{PO}_4^{3-}$  had caught up with uptake of  $\text{NO}_3^-$ . The right angle shape of the N:P ratio on Aug 12  
233 occurred as the nutriclines became sharper due to entrainment of nutrients. By Aug 13, more  
234  $\text{NO}_3^-$  was taken up at depth and the N:P ratio followed the deepening of the nitracline and  
235  $\text{PO}_4^{3-}$  was left behind. On Aug 14,  $\text{PO}_4^{3-}$  started to decrease. During Aug 10-14, a minimum  
236 in  $\text{SiO}_4^{4-}$  was present at an intermediate depth (5-10 m), coinciding with the top of the  
237 nitracline, and the silicacline followed the nitracline below 10 m.

238 **3.2. Changes in Nutrient Ratios During Field Incubations**

239 On deck incubation experiments were used to examine changes in uptake ratios by  
240 eliminating any effects due to mixing. Ambient N:P and N:Si ratios were lower at the surface  
241 than at depth, indicating higher uptake of  $\text{NO}_3^-$  at the surface. The indication of a higher  
242 uptake ratio of N:P and N:Si was supported by field incubation experiments. During nutrient  
243 addition ( $\text{NO}_3^-$ ,  $\text{PO}_4^{3-}$  and  $\text{SiO}_4^{4-}$ ) bioassays on a sample from 1 m at P3, all nutrients  
244 decreased as fluorescence increased (Fig. 7). Ambient N:P and N:Si ratios decreased to  
245 almost 0:0 after 96 h, indicating more rapid uptake of  $\text{NO}_3^-$  than uptake of  $\text{PO}_4^{3-}$  and  $\text{SiO}_4^{4-}$ .  
246 The temporal decline in the N:P and N:Si ratios resembled the temporal progression during a  
247 bloom as illustrated in C0-C3 of the conceptual profiles (Fig. 1) and in the water column (S3,  
248 P4, P6) on August 8 (Fig. 4) and during the time series at S1 (Fig. 5). During the incubation,  
249 both  $\text{PO}_4^{3-}$  and  $\text{SiO}_4^{4-}$  continued to be drawn down after  $\text{NO}_3^-$  became undetectable (Fig. 7). In  
250 an earlier incubation experiment at S3 near the end of the phytoplankton bloom on June 8,

251  $\text{PO}_4^{3-}$  was depleted at 1 m, and both  $\text{NO}_3^-$  and  $\text{SiO}_4^{4-}$  continued to disappear with 2  $\mu\text{M}$   $\text{NO}_3^-$   
252 and 4  $\mu\text{M}$   $\text{SiO}_4^{4-}$  being taken up. However, for the sample taken at 16 m,  $\text{PO}_4^{3-}$  ( $\sim 0.5 \mu\text{M}$ ) and  
253  $\text{SiO}_4^{4-}$  ( $\sim 5 \mu\text{M}$ ) continued to disappear after 1.25  $\mu\text{M}$   $\text{NO}_3^-$  was depleted after 8 h (Fig. 8).

254 The water sample at S1 on June 4 was incubated for 30 h without an addition of  
255 nutrients (Fig. 9-1). The initially low  $\text{NO}_3^-$ , and  $\text{PO}_4^{3-}$  remained near depletion levels during  
256 the incubation, but  $\text{SiO}_4^{4-}$  decreased from 9 to  $<1 \mu\text{M}$  (Fig. 9-1), which indicated that an  
257 additional 8  $\mu\text{M}$   $\text{SiO}_4^{4-}$  was taken up in excess in relation to N and P. At the end of 30 h,  
258 nutrients were added (Fig. 9-2). Both  $\text{NO}_3^-$  and  $\text{PO}_4^{3-}$  rapidly disappeared during the first 6 h,  
259 while  $\text{SiO}_4^{4-}$  decreased little (Fig. 9-2), indicating a sequential uptake of  $\text{NO}_3^-$  and  $\text{PO}_4^{3-}$  since  
260 8  $\mu\text{M}$   $\text{SiO}_4^{4-}$  was previously taken up as shown in Fig. 9A. The N:P ratio decreased faster  
261 after a single addition of  $\text{NO}_3^-$  or  $\text{PO}_4^{3-}$  alone than with additions of  $\text{NO}_3^-$  and  $\text{PO}_4^{3-}$  together  
262 (Fig. 9-3), suggesting an interaction between the uptake of  $\text{NO}_3^-$  and  $\text{PO}_4^{3-}$ . The accumulative  
263 uptake ratio of  $\text{NO}_3^-$  to  $\text{PO}_4^{3-}$  increased with time, especially when only a single nutrient was  
264 present. The ratio of N:Si decreased with time, and the accumulative uptake ratio of N:Si  
265 exceeded 3:1 in the presence of  $\text{PO}_4^{3-}$  (Fig. 9-3).

266 **4. Discussion**

267 The Strait is highly productive, reaching up to 2,700  $\text{mg C m}^{-2}\text{d}^{-1}$  in August (Yin et  
268 al. 1997b). This is due to pulsed nutrient supplies and multiple phytoplankton blooms in  
269 the shallow photic zone interacting with wind events (Yin et al. 1997b), and fluctuations in  
270 river discharge (Yin et al., 1997a; Yin et al., 1995c). Our results revealed sequential nutrient  
271 uptake to optimize nutrient uptake efficiency and generate high primary productivity by  
272 phytoplankton by taking advantage of pulsed nutrients in this highly dynamic relatively  
273 shallow photic zone.

275 **4.1. Responses of N:P and N:Si ratios to vertical mixing and uptake of nutrients**

276 A vertical profile of N:P and N:Si ratios represents a snapshot of the mixing and the  
277 uptake of N, P and Si by phytoplankton in the water column. The depletion zone of the most  
278 limiting nutrient in the euphotic zone ends at a depth where the uptake of nutrients just  
279 balances the upward flux of nutrients through the nutracline, as indicated in C3 in the  
280 conceptual profiles (Fig. 1). Different responses of nutrient uptake to pulsed nutrients by  
281 mixing appeared to depend on the previous stability of the water column, the depth of the  
282 euphotic zone and nutritional status of phytoplankton. Our observations spanned all seven  
283 conceptual profiles (Fig. 1) and indicated the dynamic processes influencing the sequence of  
284 nutrient uptake. The change in the profiles of the N:P ratio from S3 to P6 (Fig. 4) displayed  
285 the spring bloom-like progression as illustrated in conceptual profiles of C0-C3 (Fig. 1) after  
286 the wind mixing event. Various responses illustrated in the conceptual profiles C4, C5 and C6  
287 (Fig. 1) were observed in the observations, including the right angle in the N:P ratio (T7-Fig.  
288 3, P5 Aug 12, Fig. 6), parallel lines between the nutracline and the N:P ratio curve on Aug 12,  
289 (Fig. 6), and a spike in the N:P ratio curve at T11 at S1 due to continued uptake of  $\text{PO}_4^{3-}$  with  
290  $\text{NO}_3^-$  being depleted during the time period from T1 to T8 (Fig. 5), which was frequently  
291 observed on Aug 10 at P5 (Fig. 6).

292

#### 293 **4.2. Sequential Nutrient Uptake for Balanced Stoichiometry and Nutritional 294 Optimization**

295 Phytoplankton can take advantage of the dynamic mixing regimes and optimize their  
296 growth rates by taking up nutrients sequentially. The disappearance of nutrients during the  
297 incubation resembled the temporal progression of a bloom as illustrated in C0-C3 of the  
298 conceptual profiles (Fig. 1) and in the water column (S3, P4, P6; Fig. 4), or during the time  
299 series at S1 (Fig. 5).

300 Nutrient deficiency results from a decrease in the cellular content of the limiting  
301 nutrient and continuous uptake of other non-limiting nutrients. Earlier studies found that N  
302 limitation results in excess cellular content of P and Si (Conway and Harrison, 1977; Healey,  
303 1985; Berdalet et al., 1996). Some phytoplankton develop enhanced uptake of the limiting  
304 nutrient such as  $\text{NH}_4$  and  $\text{PO}_4^{3-}$  upon its addition after a period of nutrient limitation or  
305 starvation and there is an accompanying shut down of the non-limiting nutrient (Conway et  
306 al., 1976; Conway and Harrison, 1977; McCarthy and Goldman, 1979). A few hours of  
307 enhanced N uptake quickly overcomes the N debt since the enhanced uptake rate is many  
308 times faster than the growth rate (Conway et al., 1976). For example, enhanced uptake of  
309 phosphorus could double internal P within 5 min to 4 h depending on the degree of P  
310 limitation and the pulsed  $\text{PO}_4^{3-}$  (Healey, 1973). After the nutrient debt has been overcome by  
311 enhanced uptake, the uptake of non-limiting nutrients returns to normal after the cell quota of  
312 the limiting nutrient is maximal (Collos, 1986). The sequential uptake of a limiting nutrient  
313 and then the uptake of both the non-limiting and limiting nutrient is advantageous to allow  
314 phytoplankton to maintain maximum growth rates over several cell generations.

315 **4.3. Significance of Sequential Uptake of Nutrients**

316 There are two essential strategies used by phytoplankton to cope with the limiting  
317 nutrient (Collos, 1986). One strategy is the ‘growth’ response where phytoplankton uptake of  
318 the limiting nutrient and cellular growth are coupled when the limiting nutrient is available.  
319 The other strategy is the “storage” response where phytoplankton have the capability of  
320 accumulating large internal nutrient pools, resulting in extensive uncoupling between uptake  
321 and growth, and a lag in cell division of up to 24 h following a single addition of the limiting  
322 nutrient. The former strategy would have the competitive advantage under frequent pulses of  
323 the limiting nutrient, whereas the latter strategy presents an ecological advantage when the  
324 nutrient pulsing frequency is lower than cell division rate. A phytoplankton assemblage can

325 be assumed to contain both strategists in the water column. Phytoplankton species  
326 composition in subsurface waters was more or less similar at 3 stations, S1, S2 and S3  
327 considering a span of 100 km across a large salinity gradient (Clifford et al. 1992).  
328 Cryptomonads and *Chrysochromulina* spp and *Micromonas pusilla* were dominant at S2, S3  
329 and S1 in cell density (Clifford et al. 1992). The common diatom species included  
330 *Chaetoceros* spp, and *Thalassiosira* spp. (Clifford et al. 1992), which are said to use the  
331 ‘growth’ and ‘storage’ strategies, respectively (Collos 1986). At Stn S2, the chlorophyll  
332 maximum at 7 m on August 7 contained 4 times more phytoplankton cells than at the surface  
333 (Clifford et al. 1992), and was frequently observed at or associated with the nutricline  
334 (Cochlan et al., 1990; Yin et al., 1997 a). Phytoplankton there could use either the ‘growth’ or  
335 ‘storage’ strategy by different species. The storage strategy of non-limiting nutrients would  
336 allow phytoplankton to utilize the limiting nutrient when it is available and thus maximize  
337 phytoplankton growth by saving the energy expenditure associated with taking up non-  
338 limiting nutrients under limiting irradiance. This may explain why there were various modes  
339 or patterns of the N:P ratio at the nutricline, which indicates the different strategies of taking  
340 up nutrients sequentially based on the nutritional status of phytoplankton. The sequential  
341 uptake strategy allows some phytoplankton species to use the “storage” capacity for non-  
342 limiting nutrients and other phytoplankton species to use the “growth” response for the most  
343 limiting nutrient when it becomes available by mixing processes.

344 Sequential uptake of nutrients by phytoplankton can be a fundamental mechanism in  
345 maintaining high productivity in the water column where there are frequent mixing events in  
346 coastal waters. The sequential uptake strategy largely occurs at the nutraclines near or at the  
347 bottom of the photic zone. There is a consistent association between the nutriclines and the  
348 chlorophyll maximum in various aquatic environments (Cullen, 2015) and it is also common  
349 in the Strait (Harrison et al., 1991). There is a frequent upward flux of nutrients through the

350 nutricline due to entrainment in the Strait (Yin et al., 1995a, b and c) and by internal waves in  
351 the open ocean (Pomar et al. 2012). Phytoplankton in the chlorophyll maximum are generally  
352 exposed to nutrients and when these cells are brought up to the surface during entrainment or  
353 wind mixing (Yin et al., 1995a), they can quickly photosynthesize (Yin et al., 1995c). When  
354 phytoplankton exhaust the most limiting nutrient, their internal nutrient pool decreases and  
355 they sink down to the nutriclines, possibly due to the formation of clumps and take up the  
356 abundant nutrients there. Thus, the cycle of sequential uptake of limiting and then the non-  
357 limiting nutrients may reduce nutrient deficiency in phytoplankton.

358 Sequential uptake of nutrients can be an important process to maintain the  
359 phytoplankton nutrient stoichiometry. Carbon fixation continues after a nutrient becomes  
360 deficient (Elrifi and Turpin, 1985; Goldman and Dennett, 1985) and the storage of organic  
361 carbon of a higher POC:N ratio is common in phytoplankton (Healey, 1973). When  
362 phytoplankton cells with excessive organic carbon due to limitation of a nutrient, sink from  
363 the upper euphotic zone to the nutricline where light becomes limiting, uptake of other  
364 nutrients occurs by utilizing stored organic carbon, leading to an increase in the cellular N  
365 and P quotas. Thus, the ratios of carbon to other nutrients approach optimum stoichiometry.  
366 POC:N ratios at Stn S2 and S3 were observed to be between 6:1 and 7:1 in the water column,  
367 even though both ambient  $\text{NO}_3^-$  and  $\text{PO}_4^{3-}$  were near detection limits (Fig. 10). This  
368 demonstrates the lack of ambient nitrogen limitation on the cellular nutrient stoichiometry.  
369 Even at Stn S1 where entrainment and mixing were not as strong as at Stns S2 and S3, the  
370 POC:N ratio was only slightly higher than 7:1 (Fig. 10).

371 **5. Conclusion**

372 The use of in-situ continuous vertical profiles in this study shows a high variability of  
373 ambient N:P and N:Si ratios in the water column, suggesting the dynamics of nutrient uptake  
374 ratios, as illustrated in the conceptual model of Fig. 1. The incubation experiments

375 demonstrated the sequential uptake of nutrients by phytoplankton, which suggests that  
376 deficiency of a nutrient that is based on the ambient nutrient ratio could be transient and  
377 overcome by the sequential uptake of the most limiting nutrient and non-limiting nutrients.  
378 The capacity of sequential uptake of nutrients is an important strategy for phytoplankton to  
379 maintain high primary productivity and near optimum cellular nutrient stoichiometry in the  
380 water column. The sequential nutrient uptake strategy also offers another mechanism for the  
381 explanation of the variability in the nutrient stoichiometry of phytoplankton in the euphotic  
382 zone.

383 **Authors contributions**

384 K. Yin collected data and wrote the manuscript.  
385 PJ Harrison supported the research cruise for collection of data and designed the sampling  
386 plan.

387 **Competing interests**

388 The authors declare that they have no conflict of interest.

389 **Acknowledgements**

390 We thank Dr. Mike St. John who coordinated the cruise. We acknowledge the Department of  
391 Fisheries and Oceans for providing ship time, and the officers and crew of C.S.S. Vector for  
392 their assistance. This research was funded by a Natural Sciences and Engineering Research  
393 Council of Canada (NSERC) Strategic grant awarded to Prof. Paul J. Harrison. K. Yin  
394 acknowledges the continuing support of NSFC 91328203 to this study.

395

396

397 **References**

398 Armstrong, F. A. J., Stearns, C. R., and Strickland, J. D. H.: The measurement of upwelling  
 399 and subsequent biological processes by means of the Technicon Autoanalyzer® and  
 400 associated equipment, Deep Sea Research and Oceanographic Abstracts, 14, 381-389,  
 401 1967.

402 Berdalet, E., Marrasé, C., Estrada, M., Arin, L., and MacLean, M. L.: Microbial community  
 403 responses to nitrogen- and phosphorus-deficient nutrient inputs: microplankton  
 404 dynamics and biochemical characterization, *J. Plank. Res.*, 18, 1627-1641, 1996.

405 Bertilsson, S., Berglund, O., Karl, D. M., and Chisholm, S. W.: Elemental composition of  
 406 marine Prochlorococcus and Synechococcus: Implications for the ecological  
 407 stoichiometry of the sea, *Limnol. Oceanogr.*, 48, 1721-1731, 2003.

408 Brzezinski, M. A.: The Si:C:N ratio of marine diatoms: interspecific variability and the effect  
 409 of some environmental variables, *J. Phycol.*, 21, 247-257, 1985.

410 Cochlan, W. P., Harrison, P. J., Clifford, P. J., and Yin, K.: Observations on double  
 411 chlorophyll maxima in the vicinity of the Fraser River plume, Strait of Georgia,  
 412 British Columbia, *J. Exp. Mar. Biol. Ecol.*, 143, 139-146, 1990.

413 Collos, Y.: Time-lag algal growth dynamics: biological constraints on primary production in  
 414 aquatic environments, *Mar. Ecol. Prog. Ser.*, 33, 193-206, 1986.

415 Conley, D. J., Paerl, H. W., Howarth, R. W., Boesch, D. F., Seitzinger, S. P., Havens, K. E.,  
 416 Lancelot, C., and Likens, G. E.: Controlling eutrophication: nitrogen and phosphorus,  
 417 *Science*, 323, 1014-1015, 2009.

418 Conway, H. L. and Harrison, P. J.: Marine diatoms grown in chemostats under silicate or  
 419 ammonium limitation IV. Transient response of *Chaetoceros debilis*, *Skeletonema*  
 420 *costatum* and *Thalassiosira gravida* to a single addition of the limiting nutrient, *Mar.*  
 421 *Biol.*, 43, 33-43, 1977.

422 Conway, H. L., Harrison, P. J., and Davis, C. O.: Marine diatoms grown in chemostats under  
 423 silicate or ammonium limitation. II. Transient response of *Skeletonema costatum* to a  
 424 single addition of the limiting nutrient, *Mar. Biol.*, 35, 187-199, 1976.

425 Cullen, J.J.: Subsurface chlorophyll maximum layers: enduring enigma or mystery solved?,  
 426 *Annu. Rev. Mar. Sci.*, 7, 207-239, 2015.

427 Elrifi, I. R. and Turpin, D. H.: Steady-state luxury consumption and the concept of optimum  
 428 nutrient ratios: a study with phosphate and nitrate limited *Selenastrum minutum*  
 429 (Chlorophyte), *J. Phycol.*, 21, 592-602, 1985.

430 Elser, J. K., Acharya, M., Kyle, J., Cotner, W., Makino, T., Markow, T., Watts, S., Hobbie, W.,  
 431 Fagan, J., Schade, J., Hood, J., and Sterner, R. W.: Growth rate-stoichiometry  
 432 couplings in divers biota, *Ecol. Lett.*, 6, 936-943, 2003.

433 Falkowski, P. G.: Rationalizing elemental ratios in unicellular algae, *J. Phycol.*, 36, 3-6, 2000.

434 Geider, R.J. and La Roche, J.: Redfield revisited: variability of C:N:P in marine microalgae  
435 and its biochemical basis, *Eur. J. Phycol.*, 37, 1-17, 2002.

436 Goldman, J. C. and Dennett, M. R.: Photosynthetic responses of 15 phytoplankton species to  
437 ammonium pulsing, *Mar. Ecol. Prog. Ser.*, 20, 259-264, 1985.

438 Hager, S. W., Gordon, L. I., and Park, P. K.: A practical manual for the use of the Technicon  
439 AutoAnalyzer in seawater nutrient analysis, *Final Rep. Bur. Commer. Fish., Contract*,  
440 pp14-17, 1968.

441 Harrison, P.J., Parsons, T.R., Taylor, F.J.R., and Fulton, J.D.: Review of Biological  
442 oceanography of the Strait of Georgia: Pelagic Environment. *Can. J. Fish. Aquat.*  
443 *Sci.* 40: 1064-1094, 1983.

444

445 Harrison, P. J., Parslow, J. S., and Conway, H. L.: Determination of nutrient uptake kinetics  
446 parameters: a comparison of methods, *Mar. Ecol. Prog. Ser.*, 52, 301-312, 1989.

447 Harrison, P. J., Clifford, P. J., Cochlan, W. P., Yin, K., St. John, M. A., Thompson, P. A.,  
448 Sibbald, M. J., and Albright, L. J.: Nutrient and plankton dynamics in the Fraser-river  
449 plume, Strait of Georgia, British-Columbia, *Mar. Ecol. Prog. Ser.*, 70, 291-304, 1991.

450 Healey, F. P.: Inorganic nutrient uptake and deficiency in algae, *CRC Crit. Rev. Microbiol.*, 3,  
451 69-113, 1973.

452 Healey, F. P.: Interacting effects of light and nutrient limitation on growth rate of  
453 *Synechococcus linearis* (Cyanophyceae), *J. Phycol.*, 21, 134-146, 1985.

454 Hecky, R. E. and Kilham, P.: Nutrient limitation of phytoplankton in freshwater and marine  
455 environments: a review of recent evidence on the effects of enrichment, *Limnol.*  
456 *Oceanogr.*, 33, 786-822, 1988.

457 Jones, D. M., P. J., Harrison, P. J., Clifford, P. J., Yin, K., and John, M. St.: A computer-based  
458 system for the acquisition and display of continuous vertical profiles of temperature,  
459 salinity, fluorescence and nutrients, *Water Res.*, 25, 1545-1548, 1991.

460 Karl, D. M., Björkman, K. M., Dore, J. E., Fujieki, L., Hebel, D. V., Houlihan, T., Letelier, R.  
461 M., and Tupas, L. M.: Ecological nitrogen-to-phosphorus stoichiometry at station  
462 aloha, *Deep Sea Res. PT II*, 48, 1529-1566, 2001.

463 Klausmeier, C. A., Litchman, E., Daufresne, T. and Levin, S. A.: Optimal nitrogen-to-  
464 phosphorus stoichiometry of phytoplankton, *Nature*, 429, 171-174, 2004.

465 LeBlond, P.H.: The Strait of Georgia: functional anatomy of a coastal sea. *Can. J. Fish.*  
466 *Aquat. Sci.* 40, 1033-1063, 1983.

467 Loladze, I. and Elser, J.: The origins of the Redfield nitrogen-to-phosphorus ratio are in a  
468 homoeostatic protein-to-rRNA ratio, *Ecol. Lett.*, 14, 244-250, 2011.

469 Martiny, A.C., Pham, C.T. A., Primeau, F. W., Vrugt, J.A., Keith Moore. J., Levin, S.A. and  
470 Lomas, M.W.: Strong latitudinal patterns in the elemental ratios of marine plankton  
471 and organic matter. *Nature Geoscience* 6, 279-283, 2013.

472 McCarthy, J. J., and Goldman, J. C.: Nitrogenous nutrition of marine phytoplankton in

473 nutrient depleted waters, *Science*, 203, 670-672, 1979.

474 Mills, Matthew M, and Kevin R Arrigo (2010) Magnitude of Oceanic Nitrogen Fixation  
475 Influenced by the Nutrient Uptake Ratio of Phytoplankton. *Nature Geoscience* 3(6):  
476 412–416.

477 Pomar, L., Morsilli, M., Hallock, P. and Bádenas, B.: Internal waves, an under-explored  
478 source of turbulence events in the sedimentary record. *Earth-Science Reviews* 111,  
479 56-81, 2012.

480 Price, N. M.: The elemental stoichiometry and composition of an iron-limited diatom,  
481 *Limnol. Oceanogr.*, 50, 1159-1171, 2005.

482 Redfield, A. C.: The biological control of chemical factors in the environment, *Am. Sci.*, 46,  
483 205-222, 1958.

484 Sharp, J.H.: Improved analysis of particulate organic carbon and nitrogen from seawater.  
485 *Limnol. Oceanogr.*, 19, 984-989, 1974.

486 Singh, Arvind, SE Baer, Ulf Riebesell, AC Martiny, and MW Lomas (2015) C: N: P  
487 Stoichiometry at the Bermuda Atlantic Time-Series Study Station in the North  
488 Atlantic Ocean. *Biogeosciences* 12(21): 6389–6403.

489 Wood, E. D., Armstrong, F. A. J., and Richards, F. A.: Determination of nitrate in sea water  
490 by cadmium-copper reduction to nitrite, *J. Mar. Biol. Ass. U.K.*, 47, 23-31, 1967.

491 Weber, T. S., and Deutsch, C.: Ocean nutrient ratios governed by plankton biogeography,  
492 *Nature*, 467, 550-554, 2010.

493 Yin, K., Harrison, P. J., Pond, S., and Beamish, R. J.: Entrainment of nitrate in the Fraser  
494 River plume and its biological implications. I. Effects of salt wedge, *Estuar. Coast.*  
495 *Shelf Sci.*, 40, 505-528, 1995a.

496 Yin, K., Harrison, P. J., Pond, S., and Beamish, R. J.: Entrainment of nitrate in the Fraser  
497 River plume and its biological implications. II. Effects of spring vs neap tides and  
498 river discharge, *Estuar. Coast. Shelf Sci.*, 40, 529-544, 1995b.

499 Yin, K., Harrison, P. J., Pond, S., and Beamish, R. J.: Entrainment of nitrate in the Fraser  
500 River plume and its biological implications. III. Effects of winds, *Estuar. Coast. Shelf*  
501 *Sci.*, 40, 545-558, 1995c.

502 Yin, K., Harrison, P. J., and Beamish, R. J.: Effects of a fluctuation in Fraser River discharge  
503 of primary production in the central Strait of Georgia, British Columbia, Canada, *Can.*  
504 *J. Fish Aquat. Sci.*, 54, 1015-1024, 1997a.

505 Yin, K., Goldblatt, R. H., Harrison, P. J., John, M. A. St., Clifford, P. J., and Beamish, R. J.:  
506 Importance of wind and river discharge in influencing nutrient dynamics and  
507 phytoplankton production in summer in the central Strait of Georgia, *Mar. Ecol. Prog.*  
508 *Ser.*, 161, 173-183, 1997b.

509

## Figures captions

Figure 1. Conceptual model for sequential nutrient uptake, which is illustrated in vertical profiles of N, P and N:P ratios. C0 to C3 represent a time series of nutrient uptake during bloom development and C4 to C6 indicate subsequent vertical mixing of nutrients and subsequent uptake. The short horizontal line near the middle of the depth axis indicates the euphotic zone depth. N disappears first at C2, and P is left which continues to be taken up at C3. C4 represents mixing of nutrients into the bottom of the photic zone and phytoplankton have not taken up these nutrients yet. At C5, N is taken up first before P, while at C6, P is taken up first before N.

Figure 2. Map of the Strait of Georgia showing the study area and the sampling stations. Note: the Fraser River is located to the right, having two river channels flowing into the Strait of Georgia.

Figure 3. Two vertical profiles (T1=12:15 and T7=06:15) in the time series for August 6-7, 1991 of nutrients at S3. Left panel:  $\text{NO}_3^-$ ,  $\text{PO}_4^{3-}$  and N:P ratios. Right panel:  $\text{SiO}_4^{4-}$  and N:Si.

Figure 4. Vertical profiles at S3 near the Fraser River plume to P4 and P6 finally to S1 that was well beyond the plume (108 km away) during August 8, 1991. Left panel:  $\text{NO}_3^-$ ,  $\text{PO}_4^{3-}$  and N:P ratios. Right panel:  $\text{SiO}_4^{4-}$  and N:Si ratios.

Figure 5. Selected vertical profiles at S1 during the time series (T1, T3, T8 and T11) of August 8-9, 1991. Left panel:  $\text{NO}_3$ ,  $\text{PO}_4$  and N:P ratios. Right panel:  $\text{SiO}_4^{4-}$  and N:Si ratios.

Figure 6. Vertical profiles in the time series at P5 during August 10-14, 1991. Left panel:  $\text{NO}_3^-$ ,  $\text{PO}_4^{3-}$  and N:P ratios. Right panel:  $\text{SiO}_4^{4-}$  and N:Si ratios.

Figure 7. Time course of duplicate in vivo fluorescence,  $\text{NO}_3^-$ ,  $\text{PO}_4^{3-}$  and  $\text{SiO}_4^{4-}$ , and N:P and N:Si ratios during an in situ incubation of a water sample taken from 1 m at P3 on August 11 (11:45).  $\text{NO}_3^-$ ,  $\text{PO}_4^{3-}$  and  $\text{SiO}_4^{4-}$  were added to the water sample at T=0 before the incubation.

Figure 8. Time course  $\text{NO}_3^-$ ,  $\text{PO}_4^{3-}$  and  $\text{SiO}_4^-$  during the field incubation of water samples taken at Stn S3 during June 8, 1989. Top panel: sample taken at 1 m and the incubation was done under 1 layer of screening. Bottom panel: sample taken at 16 m and incubated under 4 layers of screening.

Figure 9. Time course of  $\text{NO}_3^-$ ,  $\text{PO}_4^{3-}$ , and  $\text{SiO}_4^{4-}$  during the field incubation of a water sample taken at Stn S1 on June 4, 1990. Fig. 9-1) pre-incubation: no nutrients were added to the sample during the first 28 h; Fig. 9-2) after pre-incubation, nutrients were added in 8 treatments: no additions,  $\text{NO}_3^-$  alone (+N),  $\text{PO}_4^{3-}$  alone (P),  $\text{SiO}_4^{4-}$  alone (+Si),  $\text{NO}_3^-$  and  $\text{PO}_4^{3-}$  together (+N+P),  $\text{NO}_3^-$  and  $\text{SiO}_4^{4-}$  (+N+Si),  $\text{PO}_4^{3-}$  and  $\text{SiO}_4^{4-}$  (+P+Si) and all three (+N+P+Si); Fig. 9-3) ambient and uptake nutrient ratios calculated from the time course in (Fig. 9-2). The sign "+" means "added".  $+\text{N}/+\text{P}$  and  $+\text{N}/+\text{Si}$  indicate the ratio of the added N alone over the added P alone and over the added Si alone, respectively. The uptake ratio was directly calculated from the decreasing concentrations over time during the incubation of seawater samples, e.g., using (day 2- day 1 nitrate concentration) /(day 2-day1 phosphate concentratiton) to get N:P ratio on day 1.

Figure 10. Vertical profiles of particulate organic C:N ratios at stations Stn S2, S3 and S1 along the increasing distance from the river during August 20-23, 1990.

Fig. 1

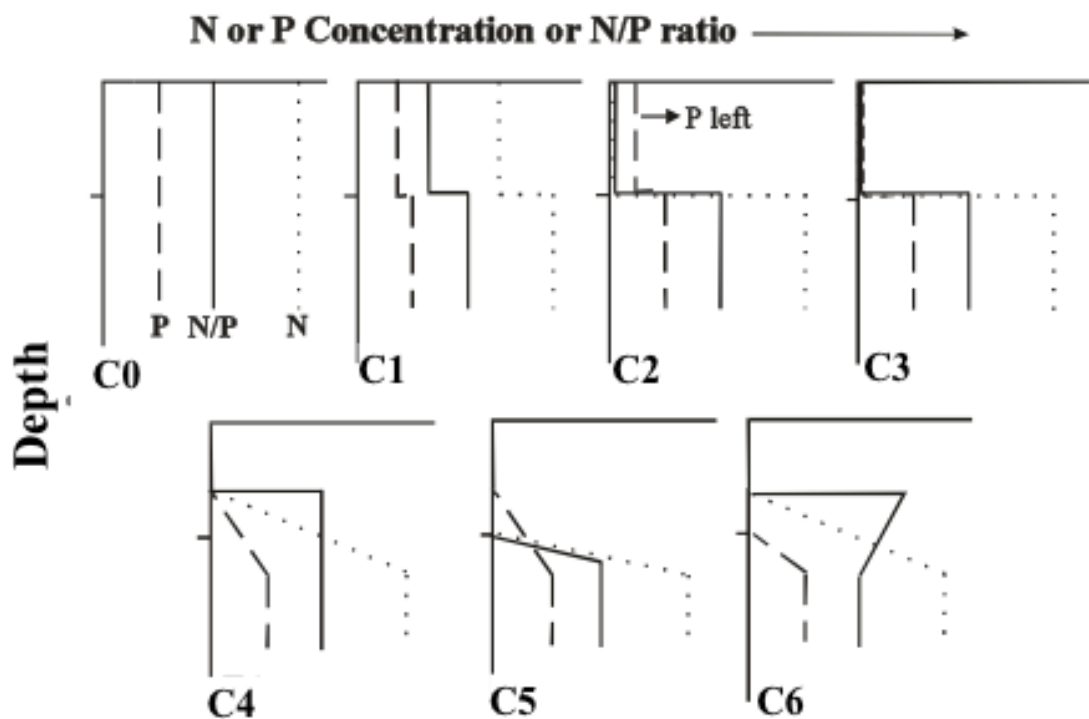


Fig. 2

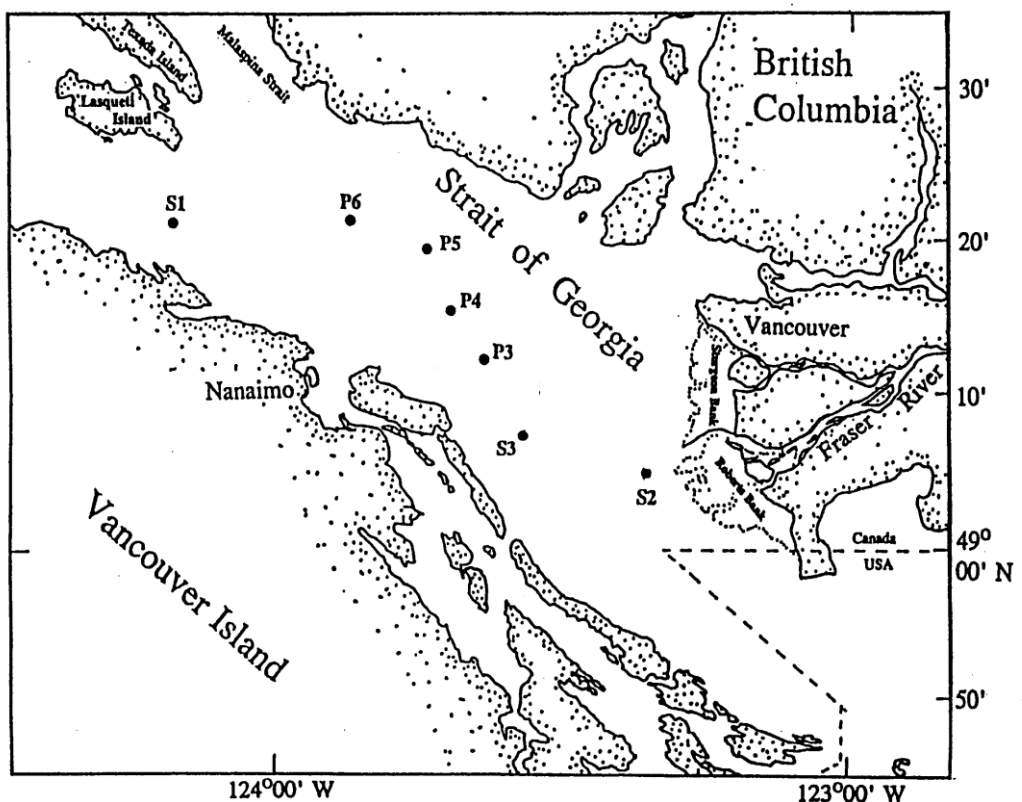


Fig. 3

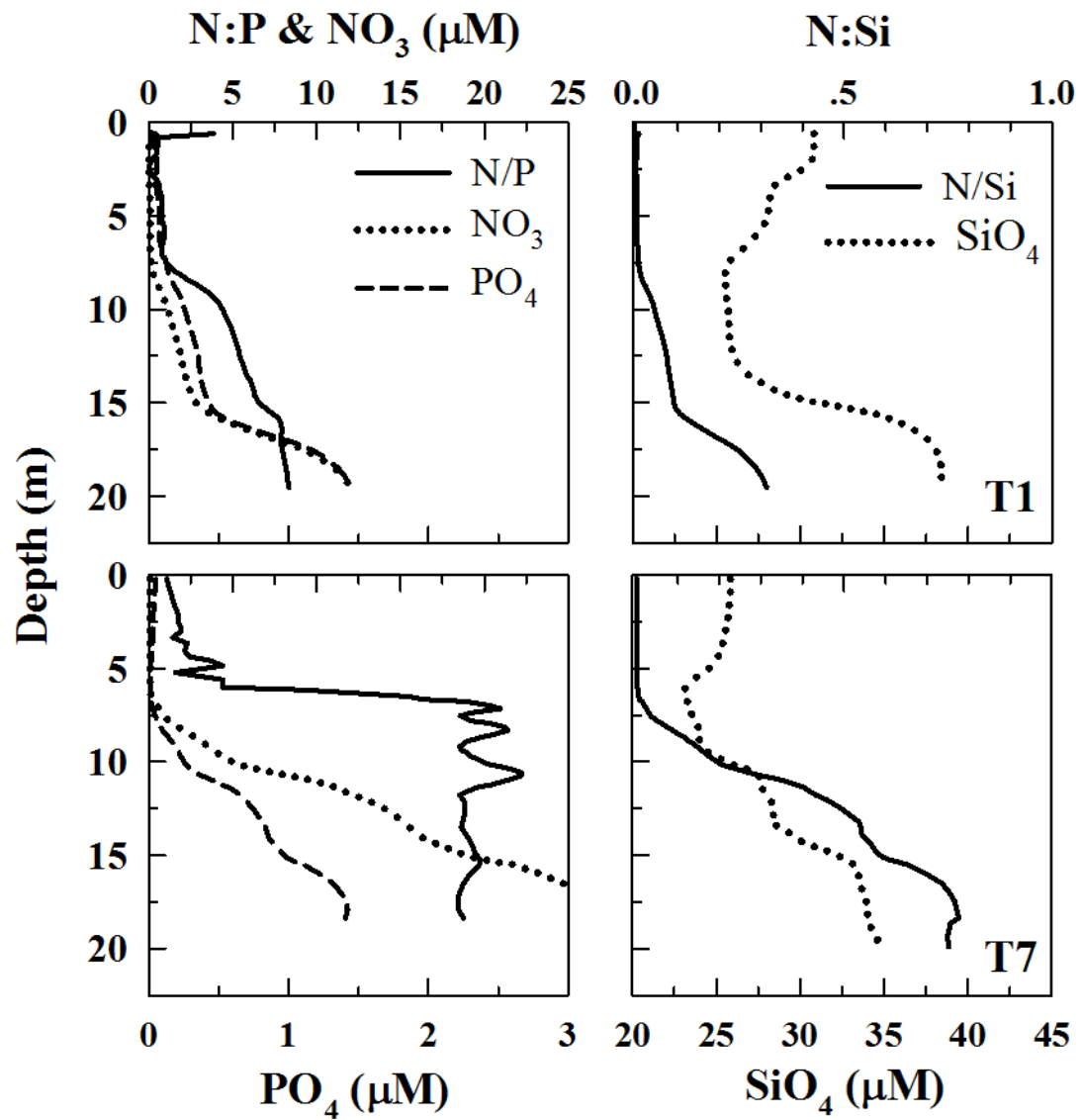


Fig. 4

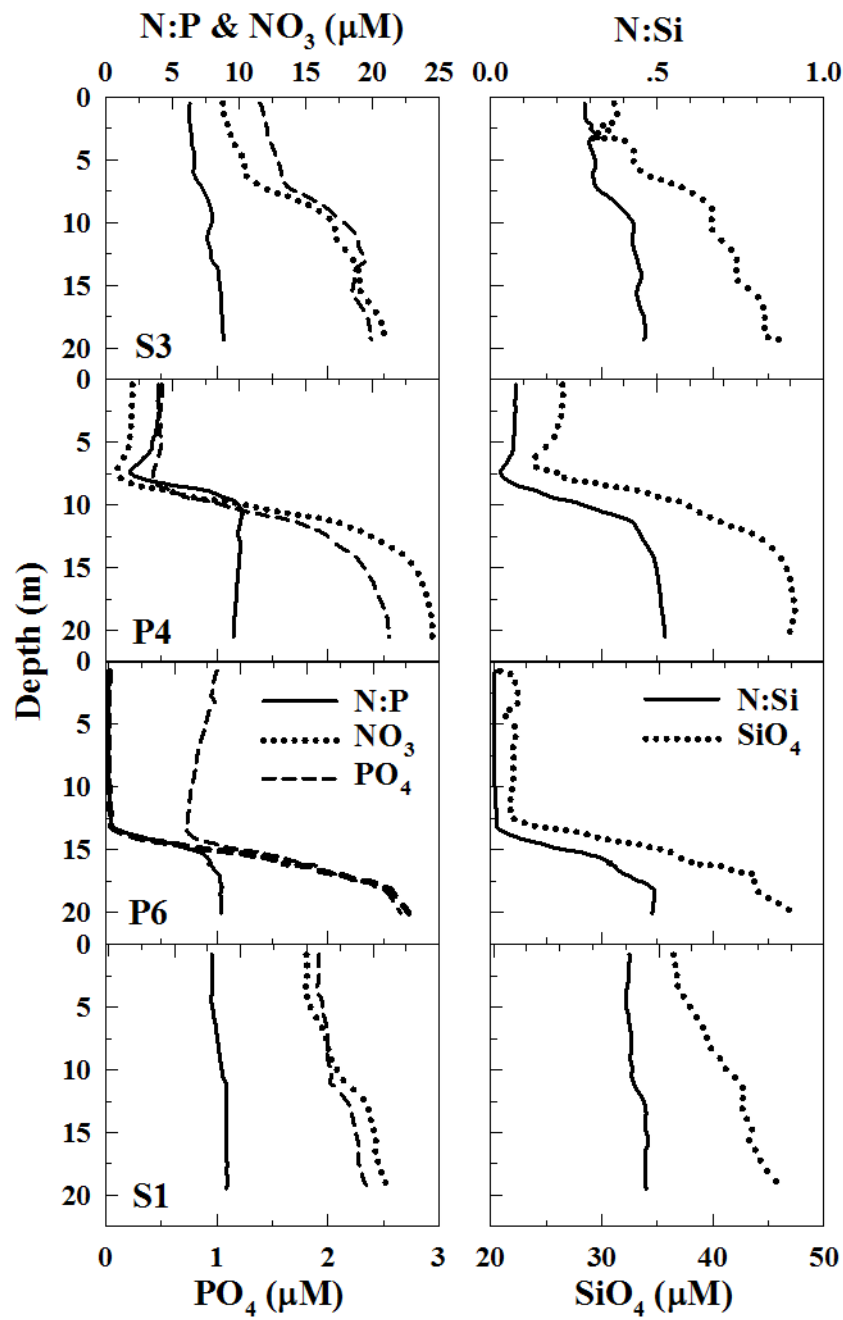


Fig. 5

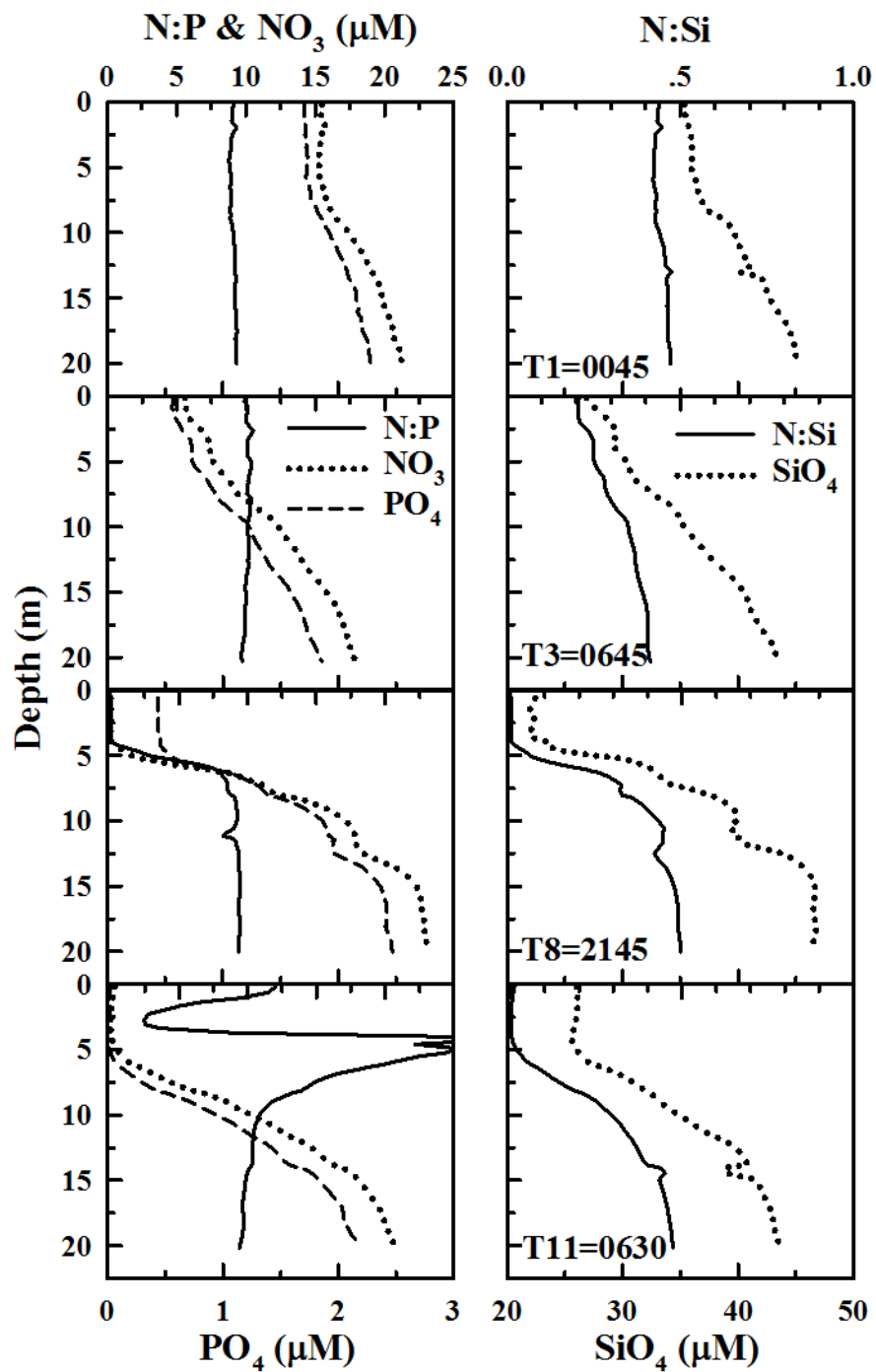


Fig. 6

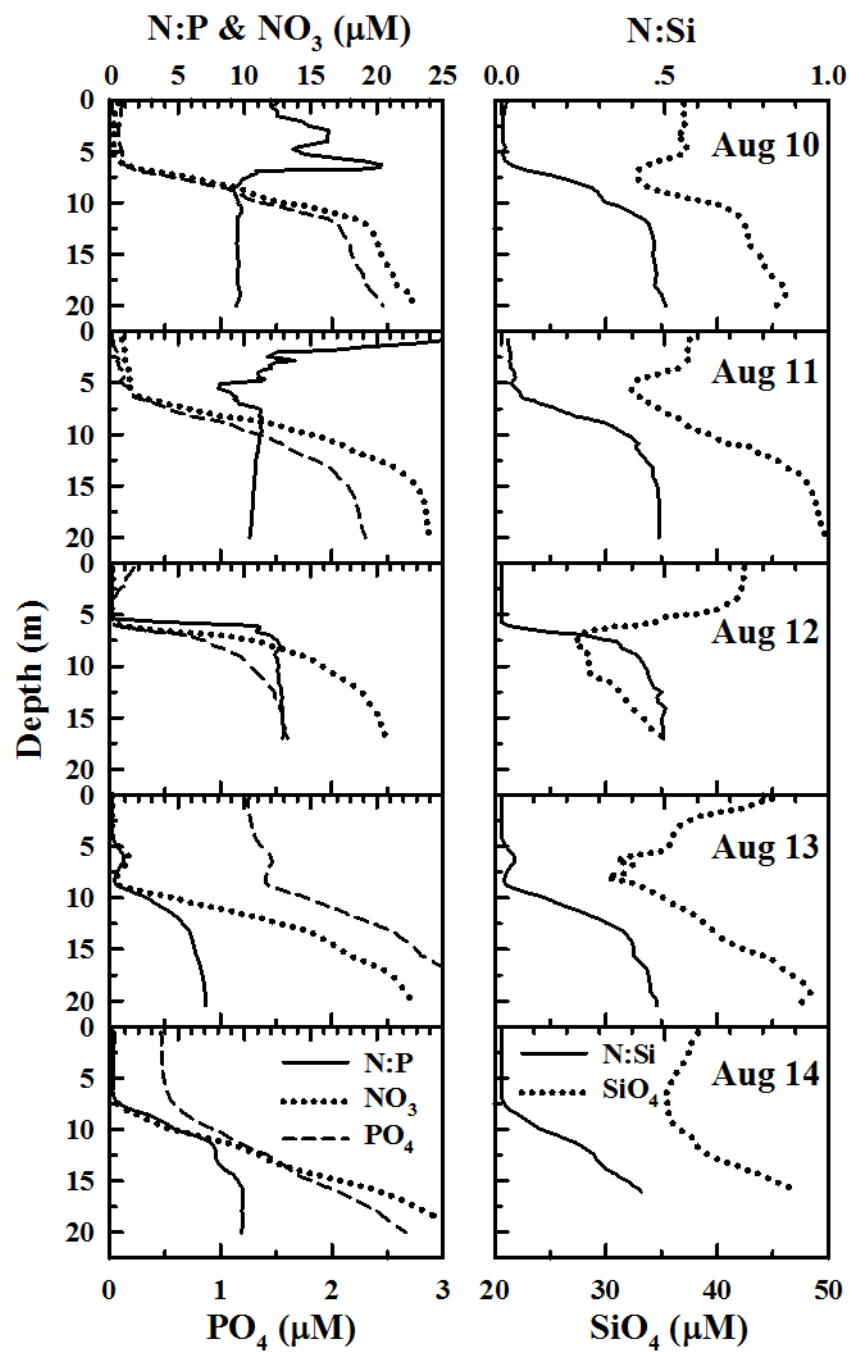


Fig. 7

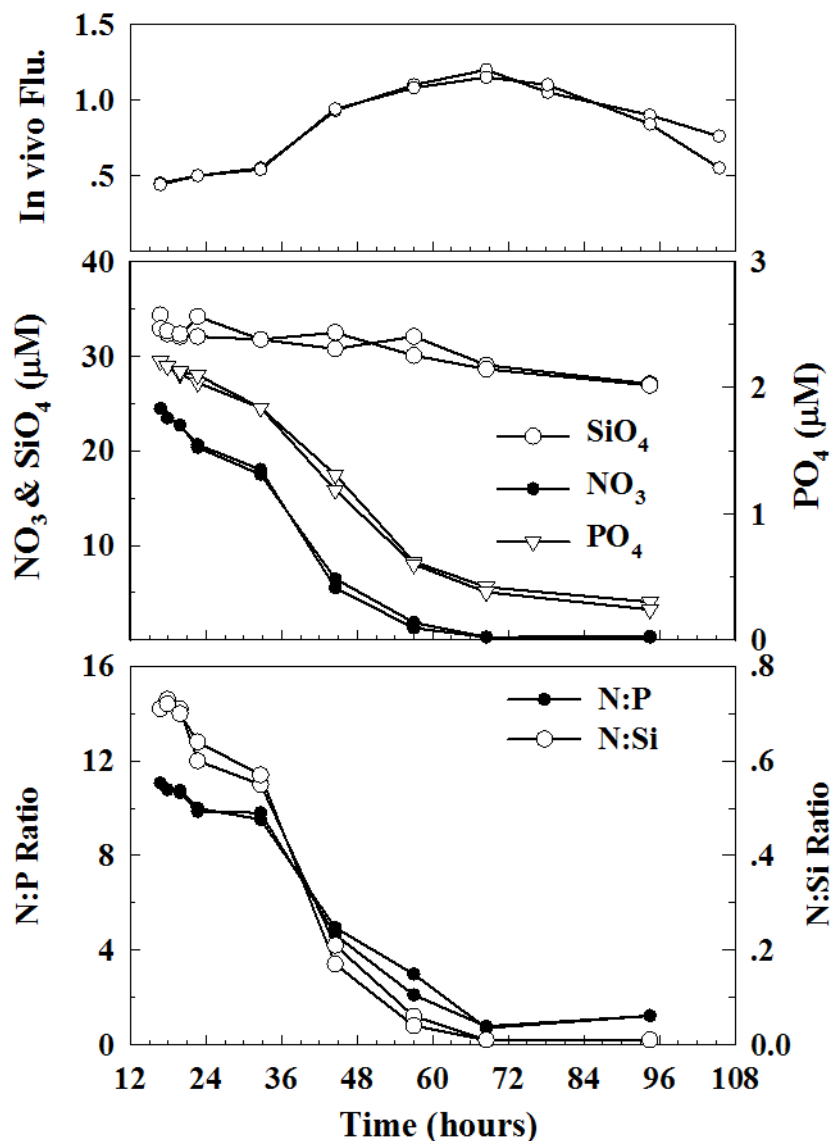


Fig. 8

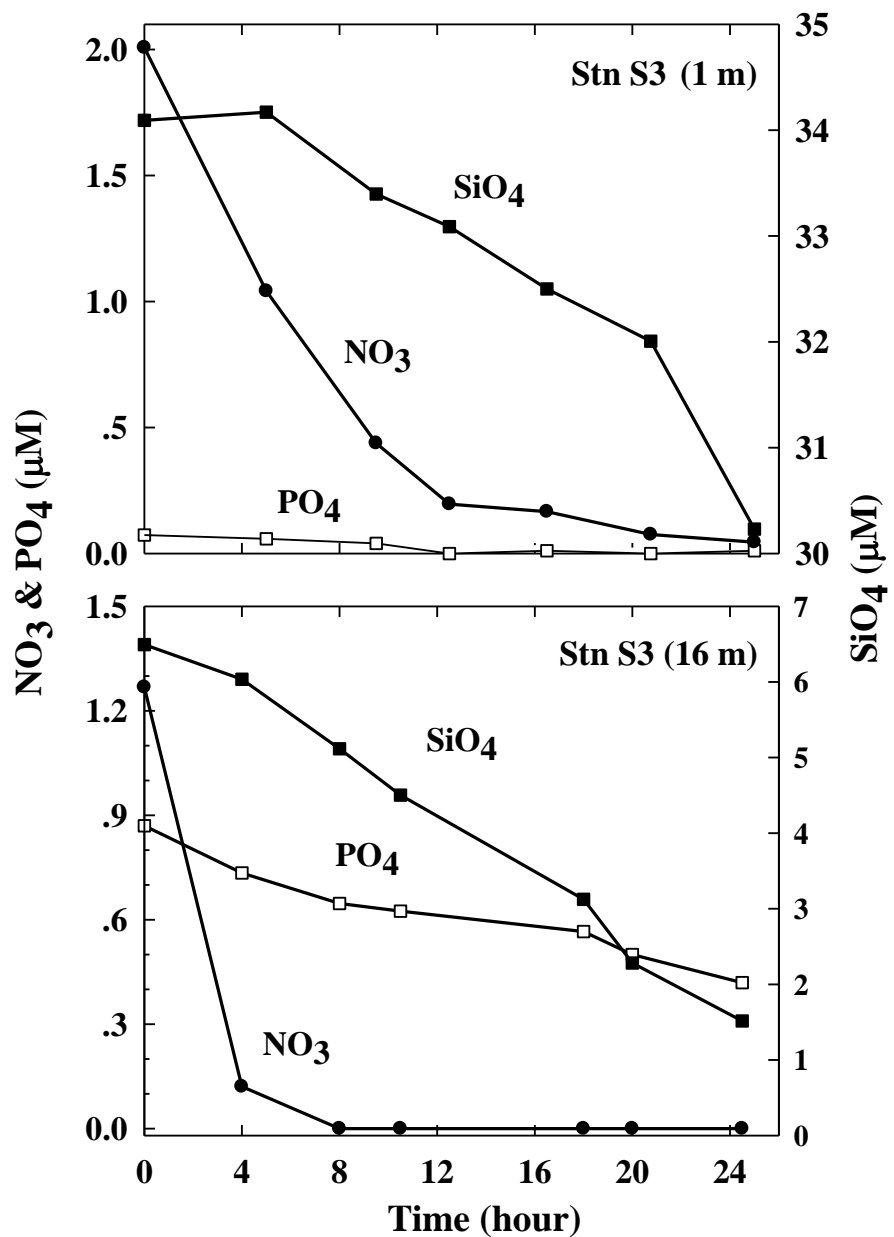


Fig. 9-1

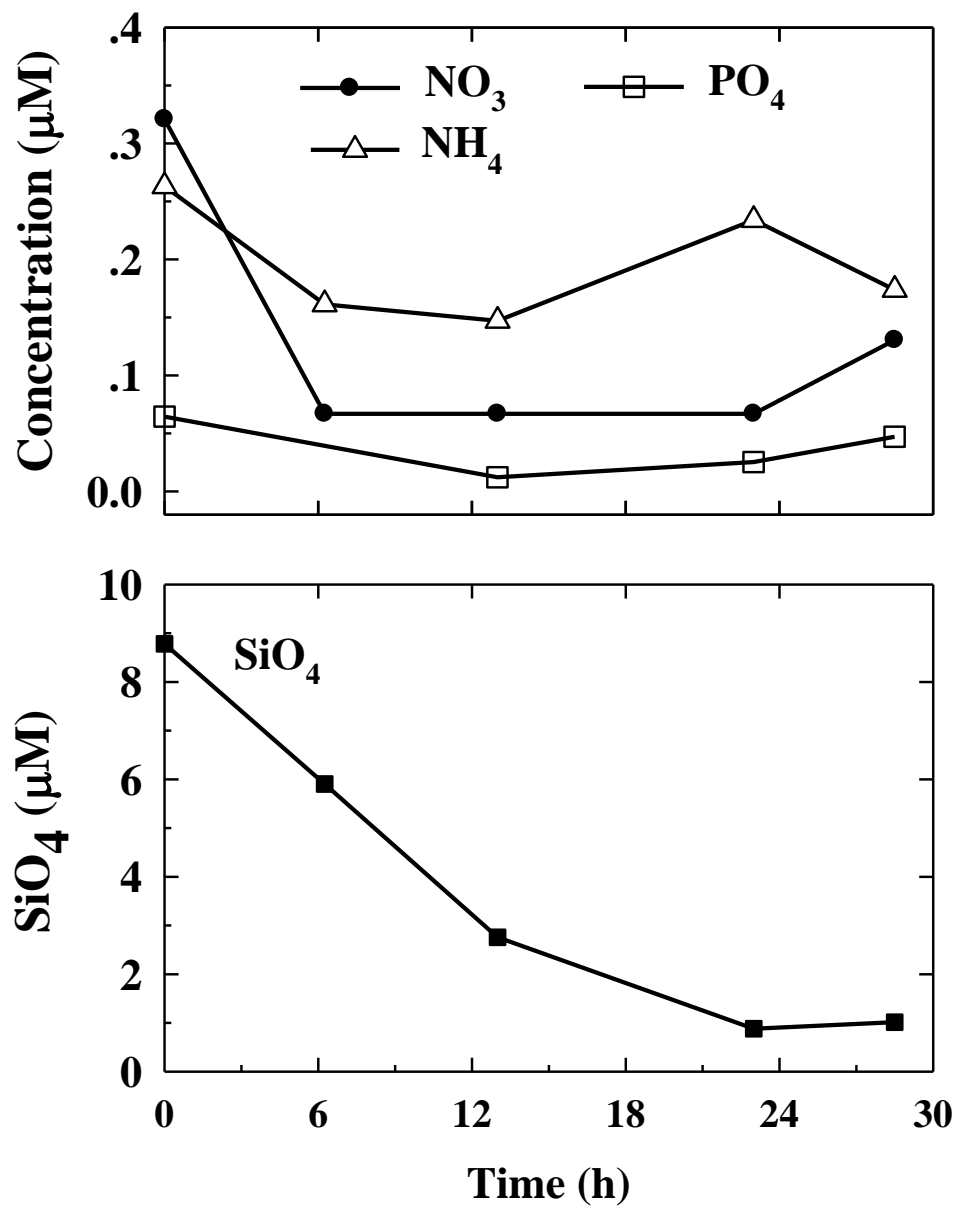


Fig. 9-2

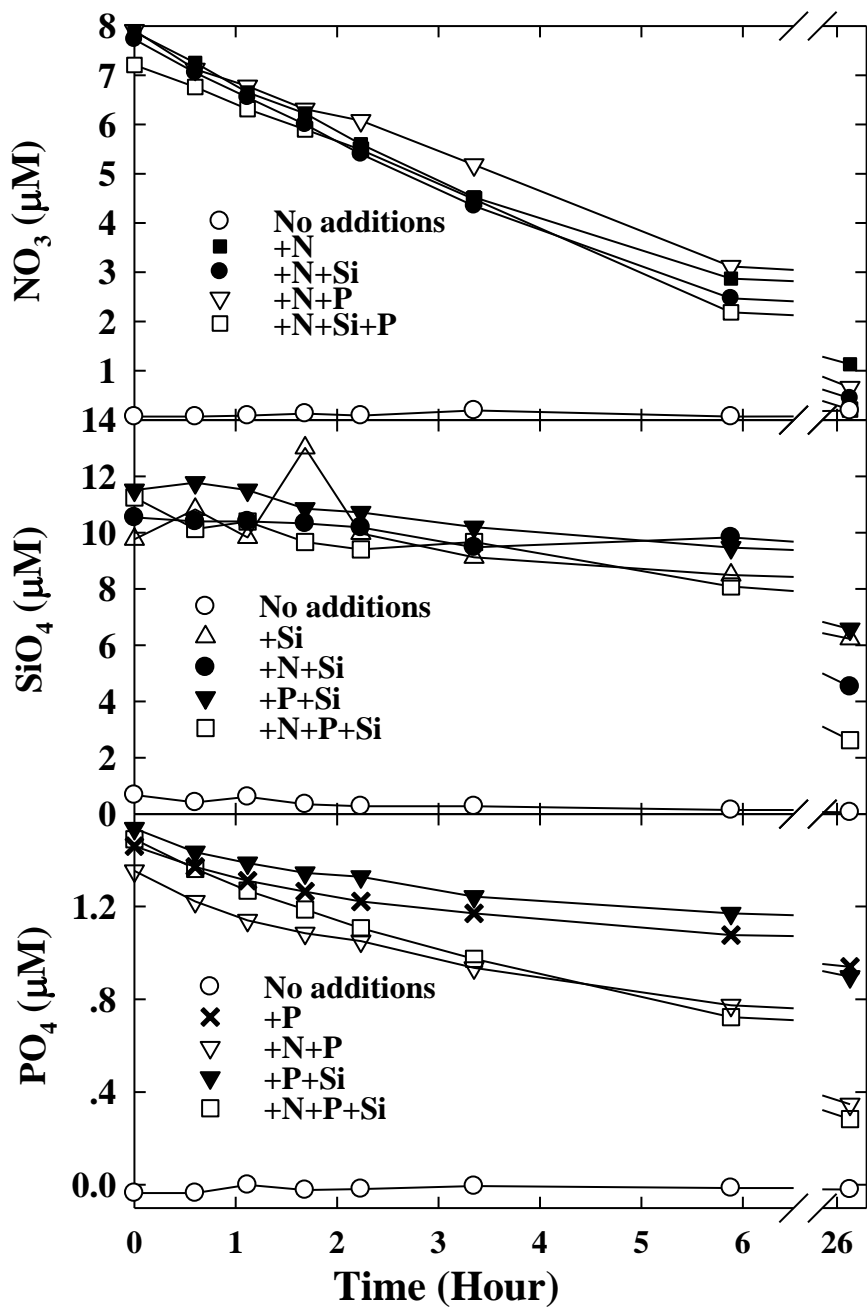


Fig. 9-3

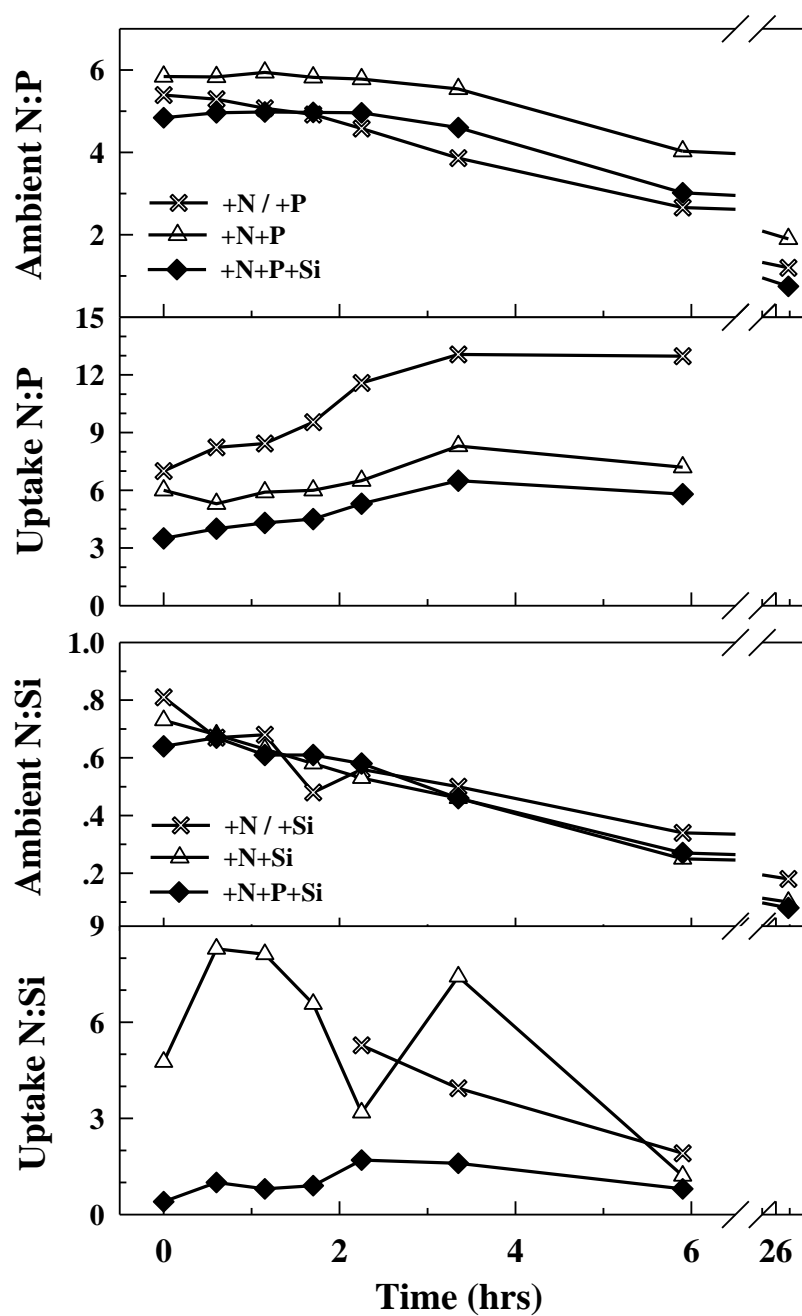


Fig. 10

